Cartesian Grid Embedded Boundary Methods for Hyperbolic PDEs

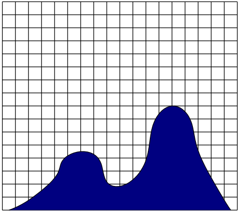

Christiane Helzel
Ruhr-University Bochum

Joined work with Marsha Berger and Randy LeVeque

Finite Volume Grids

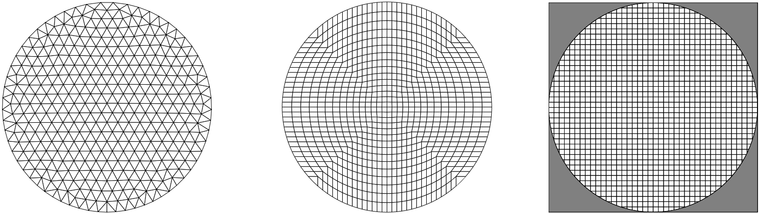

unstructured mapped cut cells

Advantages of Cartesian grid methods compared to unstructured grid methods:

- Simple grid generation / Automatic grid gereration
- Easier (more efficient) to construct accurate methods
- Simplifies the use of AMR (at least away from the embedded boundary)

Application: Cut cell representation of terrain in atmospheric models

(gravity driven geophysical flow)

Cut cell representation of orography as an alternative to terrain-following coordinate method

- More accurate computation of flow over steep hills
- More accurate computation of flow over highly oscillatory topography

Adcroft et al. (1997), Bonaventura (2000), Klein et al. (2009), Jebens et al. (2011), Lock et al. . .

Numerical Difficulty: The Small Cell Problem

Challenge is to find stable, accurate and conservative discretization for the cut cells.

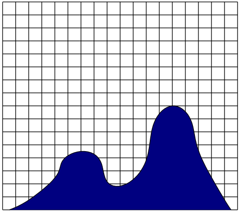

- large timestep method (LeVeque)
- cell merging
- flux redistribution (Chern &Colella)
- h-box (Berger,Helzel&LeVeque)
- mirror cell (Forrer&Jeltsch)
- kinetic schemes (Oksuzoglu; Keen&Karni)
- finite differences (Sjogreen and Peterson; Kupiainen & Sjogreen)

small cell problem - for explicit difference schemes we want time step appropriate for regular cells.

Cell Merging

Merge with nearest adjacent cell in direction normal to boundary.
(Powell et al, Quirk, Aslam, Xu & Stewart, Hunt,...)

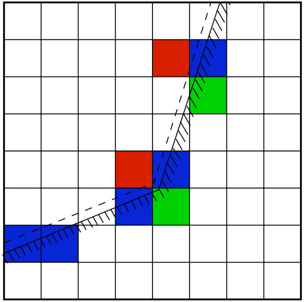

Not yet robust or automatic in 3D, complicated geometries..

Flux Redistribution (Chern and Colella)

- The usual cell update is $V_{ij} Q_{ij}^{n+1} = V_{ij} Q_{ij}^{n} + \delta M$, where $\delta M := \Delta t \sum F \cdot l$

- For small cells instead use $V_{ij} Q_{ij}^{n+1} = V_{ij} Q_{ij}^{n} + \eta \, \delta M$ where $\eta = \frac{V_{ij}}{\Delta x \cdot \Delta y}$

- $(1 - \eta)\delta M$ is redistributed proportionately to neighboring cells

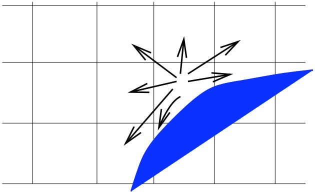

This approach can not avoid a (small) loss of accuracy in the cut-cells.

The H-box Method - 1D Case

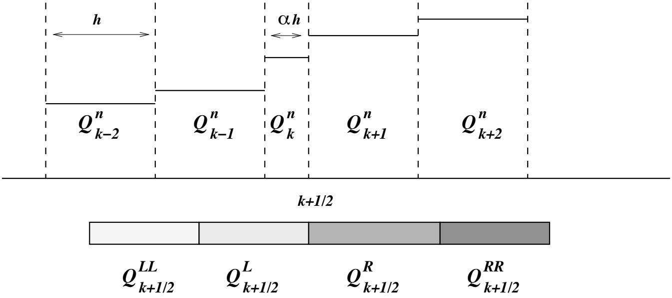

Usual method: $Q_k^{n+1} = Q_k^n - \frac{\Delta t}{\alpha h}\left(F(Q_k, Q_{k+1}) - F(Q_{k-1}, Q_k)\right)$

H-box method: $Q_k^{n+1} = Q_k^n - \frac{\Delta t}{\alpha h}\left(F(Q^L_{k+\frac{1}{2}}, Q^R_{k+\frac{1}{2}}) - F(Q^L_{k-\frac{1}{2}}, Q^R_{k-\frac{1}{2}})\right)$

Increase domain of dependence while maintaining
cancellation property: $F_{k+1/2} - F_{k-1/2} = O(\alpha h)$

H-box Method (cont)

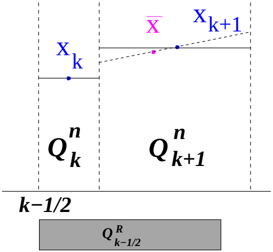

Define:

$$Q^R_{k-1/2} = \int_{x_{k-1/2}}^{x_{k-1/2}+h} Q(x)\,dx$$

$$= \alpha Q_k + (1-\alpha)(Q_{k+1} + (x_{k+1} - \bar{x})\nabla Q_{k+1})$$

pw constant: $Q^R_{k-1/2} = \alpha Q_k + (1-\alpha) Q_{k+1}$

pw linear: $Q^R_{k-1/2} = \dfrac{2\alpha Q_k + (1-\alpha) Q_{k+1}}{1+\alpha}$ (using backward diff.)

H-box method - 2D case

h-boxes in normal direction

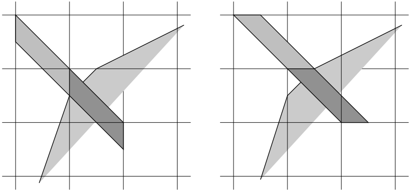

boundary h-box

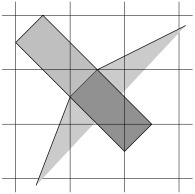

h-boxes in tangential direction

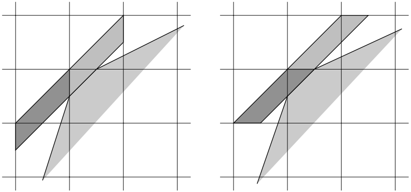

Use rotated coordinate system to maintain cancellation property

Other rotated schemes by Jameson; S. Davis; Levy, Powell and Van Leer.
First order case for advection is equivalent to Roe and Sidilkover N-scheme

We can construct cut cell methods in the context of:

- The Method of Lines (MOL)
- Predictor-corrector MUSCL type schemes

Reference: M.J.Berger and C.Helzel, A simplified h-box method for embedded boundary grids, submitted 2011.

The basic finite volume method

$$\frac{d}{dt}Q_{i,j}(t) = -\frac{1}{\Delta x}\left(F_{i+\frac{1}{2},j} - F_{i-\frac{1}{2}}\right) - \frac{1}{\Delta y}\left(F_{i,j+\frac{1}{2}} - F_{i,j-\frac{1}{2}}\right)$$

- Flux computation:

$$F_{i\pm\frac{1}{2},j} = F(Q^-_{i\pm\frac{1}{2},j}, Q^+_{i\pm\frac{1}{2},j}), \quad F_{i,j\pm\frac{1}{2}} = F(Q^-_{i,j\pm\frac{1}{2}}, Q^+_{i,j\pm\frac{1}{2}})$$

  is based on the solution of Riemann problems;

  Use (limited) piecewise linear reconstructed states;

- Use SSP-RK method in time, i.e.

$$\begin{aligned} Q^{(1)} &= Q^n + \Delta t\, L(Q^n) \\ Q^{n+1} &= \frac{1}{2}Q^n + \frac{1}{2}Q^{(1)} + \frac{1}{2}\Delta t\, L(Q^{(1)}) \end{aligned}$$

  Approximates multi-dimensional wave propagation

The 1dim H-box method (MOL)

With linear reconstruction in space and SSP-RK in time:

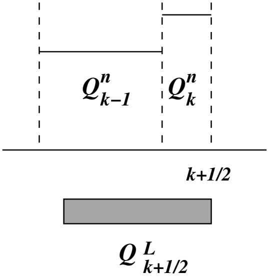

$$
\begin{aligned}
\frac{d}{dt} Q_k(t) &= -\frac{1}{\alpha h} \left(Q^-_{k+1/2} - Q^-_{k-1/2} \right) \\
Q^-_{k+1/2} &= Q^L_{k+1/2} + \frac{h}{2} \nabla Q^L_{k+1/2} \\
Q^-_{k-1/2} &= Q^L_{k-1/2} + \frac{h}{2} \nabla Q^L_{k-1/2} \\
&= Q_{k-1} + \frac{h}{2} \nabla Q_{k-1}
\end{aligned}
$$

Gradients taken from underlying Cartesian grid (using same weighting as for *h*-box values)

$$\nabla Q^L_{k+\frac{1}{2}} = \alpha \nabla Q_k + (1-\alpha) \nabla Q_{k-1}$$

The 1dim H-box method (cont.)

- Use MOL (with 2nd order SSP-RK)

$$
\begin{aligned}
u^{(1)} &= u^n + \Delta t\, L(u^n) \\
u^{n+1} &= \frac{1}{2}u^n + \frac{1}{2}u^{(1)} + \frac{1}{2}\Delta t\, L(u^{(1)})
\end{aligned}
$$

- The unlimited version is second order in space and time
- SSP gives TVD for 2nd order RK scheme if TVD for Forward Euler.
  For TVD of h-box method we need extra limiting on Cartesian grid

1D Sin Wave Test

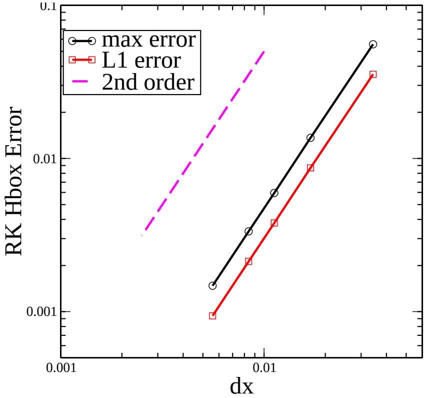

Convergence plot for linear advection for one full period, $\alpha = .1$.

The H-box Method is TVD

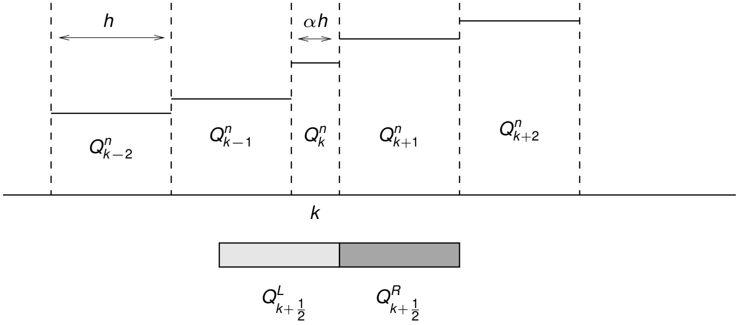

- The *h*-box method is TVD if all gradients ∇Q (includig the small cell gradient) are limited using minmod
- If the MC limiter is used, then the *h*-box method needs additional limiting either for the *h*-box gradient or the Cartesian grid gradient.

Towards the construction of higher-order *h*-box methods

$$\frac{d}{dt}\bar{Q}_i(t) = \frac{1}{\Delta x_i}\left(F_{i+\frac{1}{2}}(t) - F_{i-\frac{1}{2}}(t)\right)$$

(use 4^{th} order RK in time)

Spatial discretization is motivated by PPM of Colella and Woodward.

Regular grid case: $F_{i+\frac{1}{2}}(t) = aQ_{i+\frac{1}{2}}(t)$ with

$$Q_{i+\frac{1}{2}}(t) = \frac{7}{12}\left(\bar{Q}_i(t) + \bar{Q}_{i+1}(t)\right) - \frac{1}{12}\left(\bar{Q}_{i-1}(t) + \bar{Q}_{i+2}(t)\right)$$

(and a more complex formula on irregular grids)

The resulting method is stable for $CFL \leq 2$ and fourth order accurate.

4^{th} order accurate h-box method

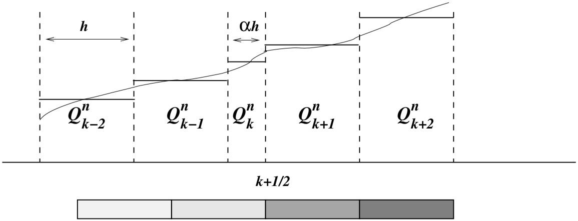

Requirements on reconstructed function $p(x)$:

1. $\frac{1}{\Delta x_i} \int_{x_{i-\frac{1}{2}}}^{x_{i+\frac{1}{2}}} p(x)dx = \bar{Q}_i,$
2. $p(x_{i\pm\frac{1}{2}}) = Q_{i\pm\frac{1}{2}} = q(x_{i\pm\frac{1}{2}}) + \mathcal{O}(h^4),$
3. $p'(x_{i\pm\frac{1}{2}}) = Q'_{i\pm\frac{1}{2}} = q'(x_{i\pm\frac{1}{2}}) + \mathcal{O}(h^3)$

Use h-box averaged values instead of cell averaged values in regular grid alg.

4^{th} order accurate h-box method: 1d advection

we get

$$(q-p)(x) = \mathcal{O}(h^4) \text{ for all } x \in [x_{i-\frac{1}{2}}, x_{i+\frac{1}{2}}]$$

$\Rightarrow$ h-box values are 4^{th} order accurate averages of the solution and can thus be used to construct 4^{th} order accurate numerical fluxes

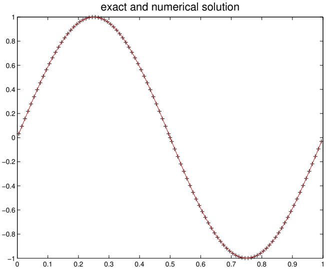

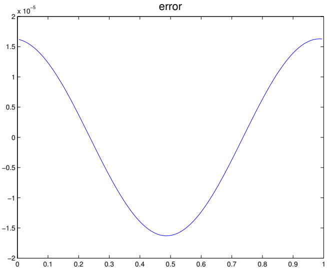

4^{th} order accurate and stable for $a\Delta t/h \leq 2$.

Multidimensional Method

Second order version

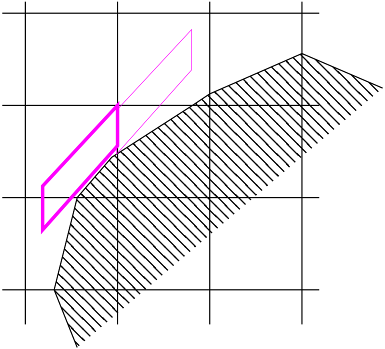

- In two dimensions each rotated box intersects at most two Cartesian cells.
- Form

$$Q_\xi^L, Q_\xi^R$$

$$\nabla Q_\xi^L = w \nabla Q_{i,j} + (1-w)\nabla Q_{i,j-1}$$

- In each direction

$$\begin{aligned} Q_\xi^- &= Q_\xi^L + \frac{\Delta\xi}{2}\nabla Q_\xi^L \\ Q_\xi^+ &= Q_\xi^R - \frac{\Delta\xi}{2}\nabla Q_\xi^R \end{aligned}$$

Multidimensional Method

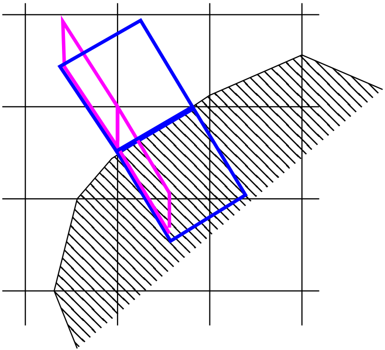

- For normal box outside domain ”reflect” to satisfy no normal flow.
- Cut cell gradients using linear least squares (also for first neighbor). Use diagonal cell if necessary.
- Limit so no new extrema at neighboring cell centers , not just face centroids (scalar minmod)

Accuracy study for advection

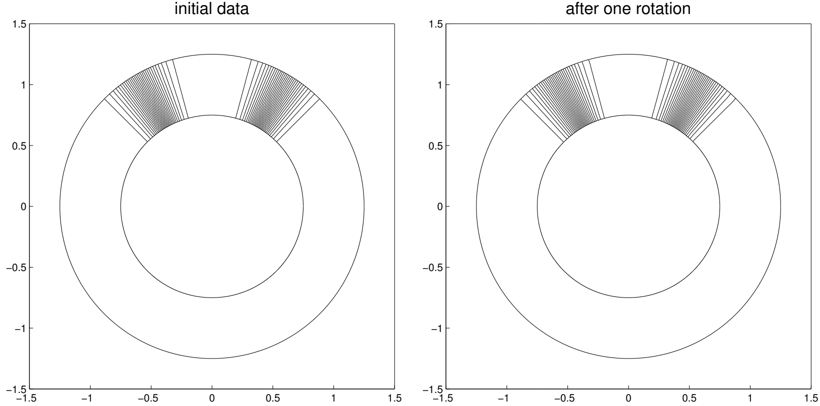

Second order accurate inside the domain and along the boundary can be achieved.

Accuracy study for advection (cont.)

Computation of error in L_1-norm:

$$E_d = \frac{\sum_{i,j} |Q_{i,j} - q(x_i, y_j)| \kappa_{i,j}}{\sum_{i,j} |q(x_i, y_j)| \kappa_{i,j}},$$

Computation of boundary error:

$$E_b = \frac{\sum_{(i,j)\in K} |Q_{i,j} - q(x_i, y_j)| b_{i,j}}{\sum_{(i,j)\in K} |q(x_i, y_j)| b_{i,j}},$$

where $|b_{i,j}|$ is the length of the boundary segment for cell (i, j).

Accuracy study for advection (cont.)

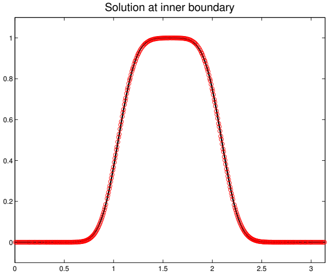

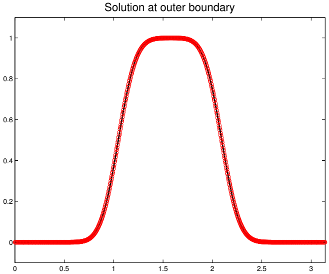

Plot of the solution in the cut cells as a function of θ after one rotation (i.e., at time $t = 5$) computed at a grid with 400×400 grid cells; (left) along the inner boundary segment which contains 780 cut cells, (right) along the outer boundary segment which contains 1332 cut cells. The solid line is the exact solution.

Accuracy study for advection (cont.)

Mesh	domain error	outer boundary	inner boundary
100×100	3.6258×10^{-2}	2.8652×10^{-2}	6.2931×10^{-2}
200×200	9.4289×10^{-2}	7.1730×10^{-3}	2.0467×10^{-2}
EOC	1.94	2.00	1.62
400×400	2.3614×10^{-3}	1.9339×10^{-3}	6.1384×10^{-3}
EOC	2.00	1.89	1.74
800×800	5.9263×10^{-4}	7.3541×10^{-4}	1.9252×10^{-3}
EOC	1.99	1.39	1.67

Table: Convergence study for annulus test problem. The h-box gradient ∇Q_ξ is computed using area weighted averaging. The rotated grid method is used only for cut cell fluxes. The time step is 0.005, 0.0025, 0.00125 and 0.000625 respectively.

Accuracy study for advection (cont.)

Mesh	domain error	outer boundary	inner boundary
100×100	2.6955×10^{-2}	1.8720×10^{-2}	4.0417×10^{-2}
200×200	7.0471×10^{-3}	4.6140×10^{-3}	1.1433×10^{-2}
EOC	1.93	2.02	1.82
400×400	1.7720×10^{-3}	1.1459×10^{-3}	3.0071×10^{-3}
EOC	1.99	2.01	1.93
800×800	4.4314×10^{-4}	2.8817×10^{-4}	7.9922×10^{-4}
EOC	2.00	1.99	1.91

Table: Convergence study for annulus test problem. The gradient ∇Q_{ξ}^{L} is computed using additional h-box values. The rotated grid method is used for all grid cell interfaces. Same constant time steps as above.

Shock reflection problem

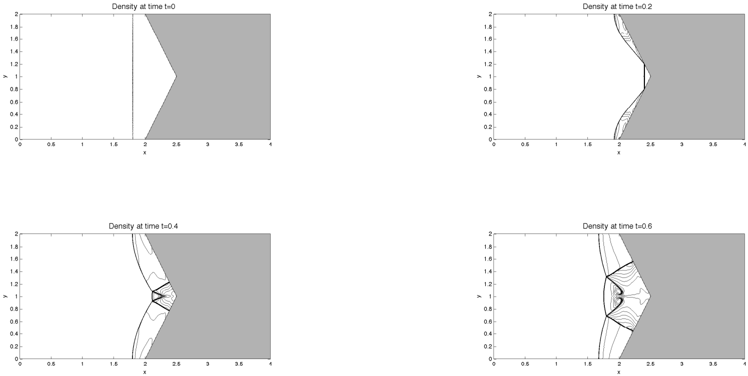

Reflection of a Mach 2 shock wave from a wedge computed on a mapped grid with 1000×1000 grid cells.

Shock reflection problem (cont.)

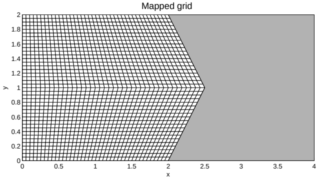

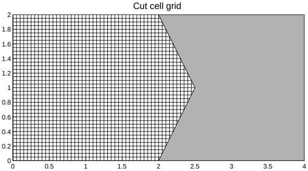

Coarse versions of the mapped grid and cut cell mesh.

Shock reflection problem (cont.)

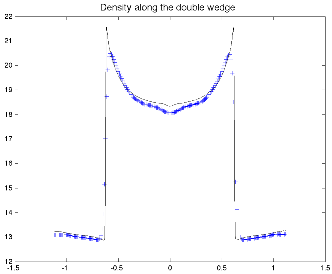

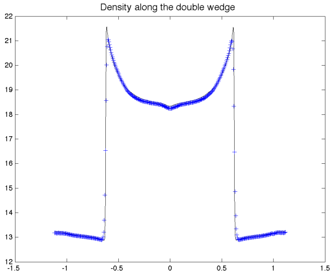

Density along the double wedge at time $t = 0.6$ computed on a **mapped grid**. The solid line is obtained from the refined reference solution. (Left) we show results from a computation using 200×200 grid cells, (right) we show results using 400×400 grid cells.

Shock reflection problem (cont.)

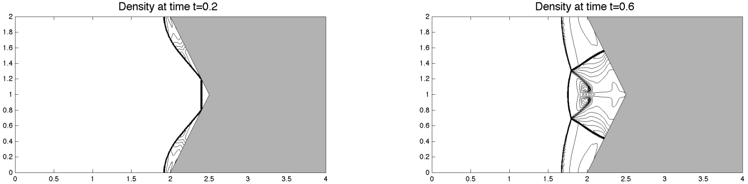

Reflection of a Mach 2 shock wave computed on a cut cell mesh with 800*x*400 grid cells.

Shock reflection problem (cont.)

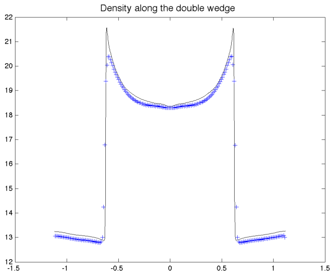

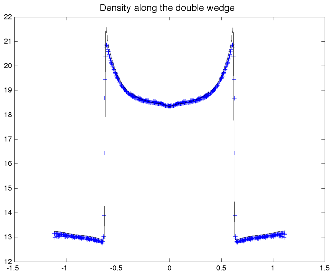

Density along the embedded boundary (cut cell values) at time $t = 0.6$.
Solid line is the density along the embedded boundary computed on mapped grid with 1000*x*1000 grid cells.

Non-smoothly varying geometry

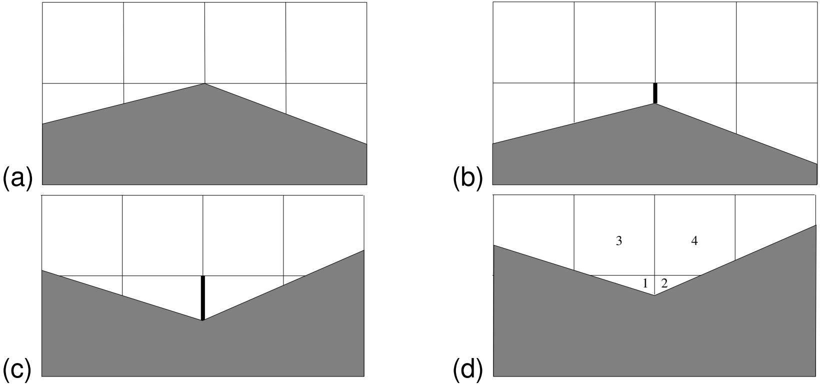

Cut cells at a convex (a)-(b) and a concave (c)-(d) non-smoothly varying boundary segment.

Conservation laws with source terms

Recall: Cancellation property (needed for stability) is based on flux difference form of the method

- Source terms can easily be included using operator splitting
- Gravity-term well balancing might be included as discussed by Botta et al. (2004) (local time-varying hydrostatic reconstruction)